Range and Contour Fused Environment Recognition for Mobile Robot

Kyung-Hoon Kim, and Hyung Suck Cho, *Member, IEEE*

Abstract– **A sensor fusion scheme for mobile robot environment recognition that incorporates range data and contour data is proposed. Ultrasonic sensor provides coarse spatial description but guarantees open space (with no obstacle) within sonic cone with relatively high belief. Laser structured light system provides detailed contour description of environment but prone to light noise and is easily affected by surface reflectivity. We present a sensor fusion scheme that can compensate the disadvantages of both sensors. Line models from laser structured light system play a key role in environment description. Overall fusion process is composed of two stages: Noise elimination and belief updates. Dempster-Shafer's evidential reasoning is applied at each stage. Open space estimation from sonar range measurements brings elimination of noisy lines from laser sensor. Comparing actual sonar data to the simulated sonar data enables data of two disparate sensors be fused at the unified feature space. Experimental results demonstrate the effectiveness of the proposed method.**

Index terms–**Environment recognition, map building, sensor fusion, Dempster-Shafer**

I. INTRODUCTION

Environment recognition for mobile robots can be defined as acquiring geometric information of surrounding objects in its own description to be used in position estimation or obstacle avoidance. Environment recognition is the most basic task required for mobile robot navigation and involves sensing and interpreting information from external sensors, thus various kinds of sensors have been devised and applied.

Among them, sonar sensor is the most widely used sensor in mobile robots due to its low cost and simplicity in manipulation. Despite of its popularity, the performance of sonar sensor is somewhat disappointing due to two problems: wide beam width and multiple reflections (also referred as specularity). A cone shaped beam width brings large uncertainty in locating target object direction, and relatively long sonar wavelength makes ordinary indoor walls or door surfaces look like mirror, which is the cause of erroneous range reading due to multiple reflections. To overcome those disadvantages, Leonard and Durrant-Whyte [1] have proposed a range data feature, the region of constant depth (RCD). From a series of range data with rotational scan of sonar, distinct sonar target objects like walls, corners and cylinders can be observed as a succession of constant range data over a certain orientation region.

Laser structured light (LSL) system is another way to obtain geometric information of surrounding environment. A laser stripe is projected horizontally onto surrounding surfaces and is observed by a camera equipped with an optical bandpass filter. Using the inverse perspective transform, world coordinates of each reflected light point can be calculated and contour information on the projected surface could be acquired. Because of its narrow beam width, LSL guarantees detailed contour information from the environment [2, 3]. However, it's likely to fail with light noise, such as sunlight, and cannot detect transparent or mirror like surfaces.

A mobile robot depending on a single external sensor is not considered as a good solution for intelligent robot system. A lot of researchers have been studying the synergistic usage of multiple sensors for mobile robots. Sonar and stereo vision [4], sonar and omni-directional vision [5], camera and laser range finder [6], and sonar and laser range scanner [7] are some of examples of pairs of sensors studied for mobile robot environment recognition. One of key advantages of the multisensor suite comes from using sensors that provide information unavailable from others [8].

Fusion methodology heavily depends on the type of sensors (also features) and goals of sensor fusion. Matthies and Elfes [4] have used Bayesian approach and occupancy grids for integration of range data from sonar and stereo vision. However, Bayesian approach cannot represent ignorance or lack of information explicitly. Dempster-Shafer's evidential reasoning is a generalization of Bayes reasoning that allows confidences to be assigned to sets of propositions rather than to just N mutually exclusive propositions [9]. Tirumalai et al. [10] have used DS reasoning for building environment maps with 3D voxels. Another alternative is a rule based sensor fusion. It can avoid the difficulty in modeling the sensor readings under a unified statistical model. Applications can be found in fusion of sonar and infrared sensors [11] and sonar and laser range finder [12].

Kyung-Hoon Kim is with Samsung Techwin, Sungnam, Korea.
Hyung Suck Cho is with Korea Advanced Institute of Science and Technology, Taejon, Korea.

In this paper, we present a sensor fusion scheme that integrates range data from a sonar and contour data from an LSL system. LCAR, a mobile robot that has been designed and built in authors' laboratory, was used as a test bed. It has two driving wheels, and a pan-tilt device on the top can make a sensor system rotate around the azimuth axis of the robot and the horizontal axis. A Polaroid ultrasonic sensor and an LSL system are mounted on the pan-tilt device. By rotating the pan-tilt device, a full 360° rotational scan of both sonar and LSL is acquired.

A single range data from a sonar sensor cannot give accurate target direction and may contain erroneous range data due to multiple reflections. However, if we extract RCDs from multiple scan data by rotating sonar, we can have more accurate description of the environment with reduced uncertainty. In this paper, we present a method to estimate an open space within the environment by classifying the type of RCDs. A detailed line description of environment contour can be acquired using LSL. However, line models from LSL may contain corrupted information from light noise and LSL cannot detect transparent or mirror like objects. Our goal is to overcome those limited sensing capabilities of each sensor by fusing two sensor data in feature level. Sonar data are used to compensate erroneous or missing contour information, while line description of the environment from the LSL enables us to get a much more detailed environment description.
Dempster-Shafer evidential reasoning is used to eliminate the fake lines from noise and update the belief of existence. However, the features obtained by each sensor are so much different that matching the same object between two sensor measurements brings another difficulty. We present a method to find the matching objects between two sensors by comparing the RCDs from actual readings and simulated readings.

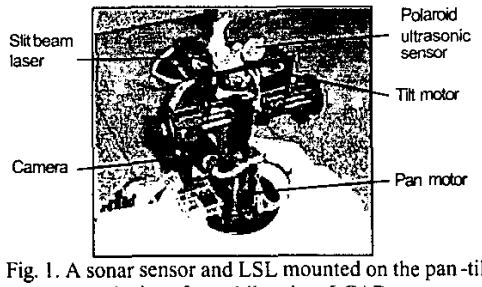

Fig. 1. A sonar sensor and LSL mounted on the pan-tilt device of a mobile robot, LCAR

In this paper, sensor fusion is performed on object-based environment description rather than on geometrical segmentations like grids [4] or voxels [10]. Grid or voxel based description split environment into same-sized boxes whose status can be either occupied or empty. In due course, the robot's behavior is limited by the resolution of its grid size. Moreover, this kind of description does not make the robot really *understand* the environment. Line and corner models used in this approach can provide not only geometrical but also topological description of the environment. Thus, more intelligent and advanced robotic navigation problems can be followed.

II. GEOMETRIC FEATURES OF SONAR AND LSL

A. Region of Constant Depth

Polaroid ultrasonic sensor, which is the most widely used sonar sensor between mobile robots, has a visibility angle of about 25°. When a range data is acquired, it means a target object whose distance from the sensor equal to the range value exists within the sensor's visibility cone. In other words, we have about 25° of uncertainty on the target's directional angle. This uncertainty can be much reduced if we take a rotational scan (acquiring range data at the constant step angle) of the environment. Region of constant depth (RCD) is a connected set of sonar returns with constant range data, and it is a sensor feature that can be acquired only from distinctive objects like wall, corner, edge and cylinder. Leonard and Durrant-Whyte[1] have extensively studied on RCDs and successfully used them in localization and navigation. Fig. 2 shows a typical sonar scan of an environment composed of walls and corners, and the RCDs obtained from the scan.

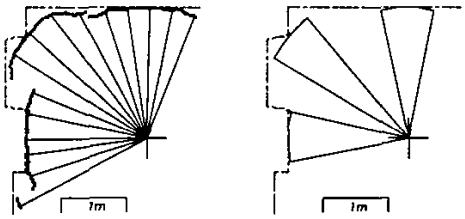

Fig. 2. Actual sonar scans in a room and RCDs obtained from the scan. RCDs are obtained from sonar reflections less than 1.0 cm of range difference and more than 10 degree of continuity. Dashed line is hand measured room contour. Time-of-flight (TOF) dots are shown for every return, and rays are drawn at every 10th return.

The width of an RCD describes how strong the echo is. When a strong echo is received and other objects do not occlude the target, the width of an RCD almost equals the visibility angle of the sonar sensor. However, the width of RCD depends largely on the layout of objects rather than the type of objects. Thus, the difference in width of RCDs cannot give enough clues to recognize the target type.

From observing the sonar scan in a real world environment, we could find out that RCDs can be categorized into four different types according to the relationship with the adjacent range data. Fig. 3 explains four different RCD types. Type I is an RCD with an average range data shorter than adjacent range data in both left and right sides. This type of RCD appears when the target object is closer than neighboring objects. Usually this kind of RCD shows the

largest width due to the strong echo. Because we measure the range by time-of-flight (TOF) of the first echo only, this type of RCD means that an echo reflection point lies within the RCD and the point is closer than any other object within the RCD. One of major disadvantages of sonar is its wide beam width so that it cannot locate the accurate target direction. But inversely it means that we have a strong belief that no other object than the target exists, i.e. an open space, within a Type I RCD. Thus, an open space assumption can be made over the entire area of a Type I RCD. However, when a multiple reflection happens over surrounding walls, open space is not guaranteed over the entire area. Multiple reflections usually accompanies a big range jump or a range reading equal to the maximum detectable range, which is a design factor of the timing circuit for sonar. Thus, a multiple reflection can be identified from a range data difference larger than a certain threshold or range data equal to the maximum range. This type of RCD is classified as a Type IV, and no open space assumption can be made.

Type II RCD is an RCD neighboring a shorter-range data in one side and a farther range data in the other side. While the echo reflection point lies within the arc of Type I RCD, Type II RCD may have the reflection point lying out of the arc of RCD, because wide visibility angle makes other nearer targets detected even when it's facing a target. RCDs of this kind are mostly observed from small corners (or edges) which can be seen at small extrusions or recesses in real world environments. Due to the multiple reflections in large incident angle, the arc of Type II RCD cannot represent the open space like Type I RCD. However, we can expect an open space within Type II RCD area up to the range equal to the shorter adjacent range reading.

Type III RCD is the opposite one of Type I RCD, i.e. an RCD neighboring shorter-range readings in both sides. This type of RCD can be observed from pathway to open space, like corridor. However, this type of RCD also appears as a result of multiple reflection from smooth surfaces. Thus, an open space within the RCD can be expected only up to the range equal to the shorter neighboring range reading.

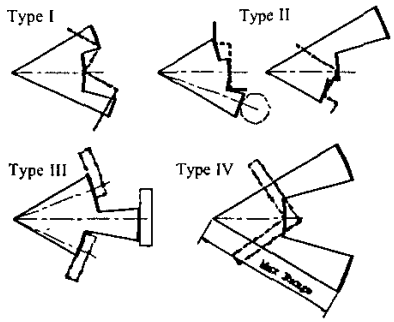

Fig. 3. Different types of RCDs

While conventional RCD identification considers only RCDs with large width, open space assumption is independent on the width of RCDs. Even an RCD with a single sonar reading can be used to get the open space within an environment. Thus, we define a term, primitive RCD, which is an extended RCD that does not have a minimum requirement on the width.

B. Line Model

LSL uses a horizontal laser slit beam to detect the contour of the surrounding environment. Thus, line model can be considered as the most suitable form of environment description for LSL. Gonzalez et al.[13] have demonstrated usefulness of line models in map building for mobile robots with a 2D time-of-flight laser rangefinder.

Line model of environment from LSL can be acquired from a series of image processing of acquired image. At the image level, preprocessing of an image with line mask convolution and binarizing with maximum intensity over a threshold enhances laser line image. Polyline approximation from the acquired binary image extracts line segments. Finally, triangulation implemented by inverse perspective transform makes us calculate the corresponding world coordinates of endpoints of line segments [14].

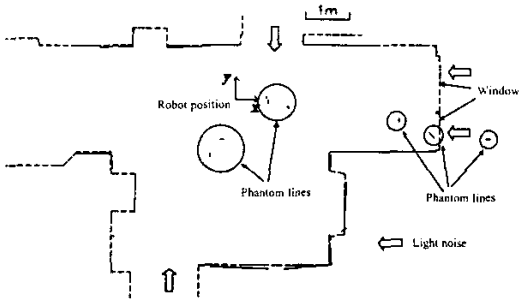

Fig. 4. Acquired line map (solid lines) using LSL superposed on the hand measured contour (dashed lines) of a corridor.

The width of laser line on the projected surface within the desired range (about 7 or 8 meters) can be easily maintained at several millimeters and reflected image can be observed over a wide range of incident angle. Thus, LSL can provide a good spatial resolution for environment recognition of mobile robots. For LSL installed on LCAR with a camera having about 27 degree of field-of-view (FOV), 15 snap shots at 24deg step angle are required to cover a full circle. An example of line model acquisition in an indoor environment, as shown in Fig. 4, shows LSL provides quite a good description of the environment. However, LSL cannot detect a transparent object like windows. The LSL successfully detected a wall at the bottom of Fig. 4, but there is no single line segments acquired from two windows in the right side. Also, the acquired line models are corrupted with erroneous line models by a light noise from sunlight coming through the window. Even though LSL uses a laser light that has a very narrow spectrum and an optical band-pass filter and LSL has its own noise rejection

algorithm, that eliminates very short line segments, sunlight coming through the windows adds noisy lines in the acquired line map. Moreover, modern buildings are more filled with glasses than before. This inability becomes a major disadvantage for LSL to be used in natural indoor environments.

III. FUSION OF RANGE AND CONTOUR

In our method, the line map acquired from LSL plays a major role in environment recognition. RCDs acquired from sonar sensor cannot give enough spatial resolution that can be acquired with line models from LSL. However, phantom lines from light noise and undetectable transparent objects are major problems for LSL. These problems can be resolved by integrating line model of the environment with sonar range data. Moreover, fusion of two sensors provides a belief reinforcing mechanism of the acquired environment models. The overall environment recognition process is composed of two stages: (1) Noise elimination and smoothing of line maps, and (2) belief reinforcement of acquired line models. The Dempster-Shafer's (DS) evidential reasoning method is used in both stages.

Dempster's rule of combination [15] provides a method for combining two evidences assigned to propositions of interest m_1 and m_2 obtained from two independent sources to produce an updated evidence m_{12} that represents a consensus of the two sources. Mathematically, it is represented as:

$$m_{12}(C) = \frac{\sum_{\substack{A,B\subseteq\Theta \\ A\cap B=C}} m_1(A)m_2(B)}{1-\sum_{\substack{A,B\subseteq\Theta \\ A\cap B=\phi}} m_1(A)m_2(B)} \qquad (1)$$

where A, B and C corresponds to the set of propositions of interest. In noise elimination stage, m_1 and m_2 would correspond to the basic probability assignment (*bpa*) of sonar sensor and LSL, respectively. The set of proposition for sonar A can be defined as $\{Real, Noise, Unknown\}$. The *bpa* for each proposition can be evaluated from the relationship with the open space, acquired from the RCD type classification of sonar scan data. The set of proposition for LSL B can be defined as $\{Real, Unknown\}$. LSL does not have any method to evaluate whether an extracted line is from real object or light noise. Thus, the state *Noise* cannot be acquired from LSL.

The relationship with a line segment model and the open space acquired from sonar data can be categorized into three states: (1) completely outside the open space, (2) partly inside the open space, and (3) completely inside the open space. When the line segment is contained completely outside of the open space, we would have a stronger belief that it's a real object rather than it's a noise. Oppositely, when the line segment is completely inside the open space, we would have a stronger belief in noise than real object. When the line segment is partly inside the open space, we would say that it's hard to distinguish. Considering these *a priori* knowledge, we have assigned *bpa* from sonar sensor m_1 as shown in Table 1. For *bpa* from LSL m_2, we would have a stronger belief on *Real* as the length of line segment increases, because lines from noise tends to be short in length. We have defined a *bpa* function for m_2 as follows:

$$\begin{aligned} m_2(\text{Real}) &= c\cdot\frac{l}{L} \quad (l \le L), \\ &= c \qquad (l > L), \\ m_2(\text{Unknown}) &= 1 - m_2(\text{Real}), \end{aligned} \qquad (2)$$

where l represents the length of line segment in world coordinates, and L and c are constants that control the variable range of the *bpa*.

Table 1. Basic probability assignment for noise elimination

Sensor	Relationship with open space	Basic probability assignments
Sonar	Completely outside	$m_1(\text{Real}) = 0.8$ $m_1(\text{Noise}) = 0.1$ $m_1(\text{Unknown}) = 0.1$
	Partly inside	$m_1(\text{Real}) = 0.1$ $m_1(\text{Noise}) = 0.1$ $m_1(\text{Unknown}) = 0.8$
	Completely inside	$m_1(\text{Real}) = 0.1$ $m_1(\text{Noise}) = 0.8$ $m_1(\text{Unknown}) = 0.1$
LSL	-	$m_2(\text{Real}) = c\cdot\frac{l}{L}$ $(l \le L)$, $= c$ $(l > L)$, $m_2(\text{Unknown}) = 1 - m_2(\text{Real})$, ($c = 0.6$ and $L = 40$cm)

Combined evidence of existence is calculated using equation (1) for each line segment and lines with more evidence in *Noise* than a specific value (for example 0.5) would be considered as a noise and eliminated from the map.

Though lines from light noise are eliminated, still the acquired line map is composed of a series of short line segments due to small FOV of camera and image overlapping occurred in rotational snapshots. For further updates of environment models, merging of these line segments to reduced line description is also required. A pair of lines whose end points lie within a tolerance boundary of the other and whose difference in slop angles is within a tolerance are merged together. After merging of small line segments, edge and corner points are found by comparing the distances between end points of all line segments. For a pair of lines whose end points lie within a tolerance circle are considered to meet together at the midpoint between two end points. Consequently two end points of the pair of lines are modified to that corner (or edge) point. In this way, we can have a complete and simplified environment model composed of lines and corner points without any loss of information.

The last step of sensor fusion is the updates of the acquired map elements. Those objects observed simultaneously from both sensors would have a reinforced evidence of existence. Objects detected by only one of two sensors would have

mid-level evidence. Lines observed by LSL but not by sonar and transparent objects detected by sonar but not by LSL could be examples of those objects. One difficulty arises here in finding the matching target between sonar and LSL. Due to the large uncertainty in direction angle of sonar target, it is difficult to distinguish the target from the acquired line-corner map. Thus, we generated a simulated sonar scan from the acquired line-corner map using a simulation model of sonar sensor. The simulated sonar data will represent the measured environment by LSL rather than by actual sonar. Thus, we can compare measured data from two independent sources in the same feature space.

Kuc and Siegel [16] studied an analytic model based on the impulse response and suggested a simulation model of ultrasonic sensor. Their work has been considered as a good reference for most of researchers who have studied application of sonar sensors. Leonard and Durrant-Whyte [2] used the sensor simulation model in fusing sonar sensor measurements with odometry data to solve the localization problem. We also use this simulation model to get the simulated sensor readings from the acquired line map.

After generating simulated sonar scan from the acquired line-corner model, RCDs are extracted with the same method used in RCD extraction from actual sonar readings. Matching RCDs from simulated scan and those from actual sensor readings can be found by comparing the direction angle and average range data of every RCD, which are two major features of RCDs. RCDs showing nearest distance in two features would be selected as a matching pair. In the simulation model, we can identify which is the correct sonar target of current sonar reading. If the identified sonar target appears to be a line (a wall in real environment), belief of that specific line will be reinforced. However, when the identified sonar target appears to be a corner or edge, it also supports the belief of two line segments surrounding the corner. Thus, the belief level of those two lines would be reinforced.

IV. EXPERIMENTAL RESULTS

Fig. 5 (a) shows actual sonar scans obtained from the same environment shown in Fig. 4. Range data plot represents the actual contour relatively well in most of places. However, spurious range data due to multiple reflections (marked as SR) can be observed at the wall of the bottom side of right end space and the wall at the left top side. Very long range reading above the robot position is a typical Type III RCD, which can be observed at the passage way to another open area. Please note that windows undetected by LSL at the right end of corridor could be observed by sonar. After classifying the type of RCDs, open space area is obtained as shown in Fig. 5 (b). The obtained open space from the sonar well represents the actual open space, except the wall marked, where we got the mu ltiple reflection.

26 of total 28 fake lines from light noise could successfully be eliminated by DS based sensor fusion. Only two fake lines observed near the window at the right end side of Fig. 4, could not be eliminated, because they were completely out of bound of estimated open space. Line merging and corner finding from the noise-eliminated line map was followed. 62 line segments (excluding 26 deleted fake lines) in original line map were reduced to 42 lines with the distance tolerance of 5cm and angular tolerance of 10°. From merged line map, 14 corner points were found with the distance tolerance of 5cm.

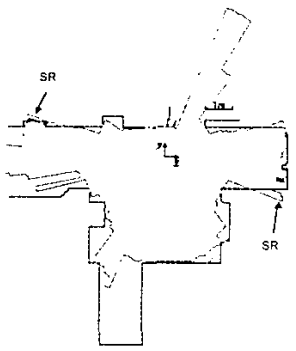

(a) Raw range scans taken by the rotating sonar

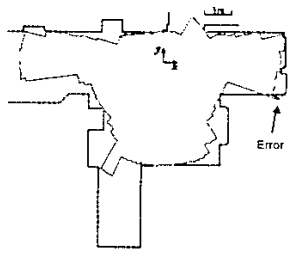

(b) Open space estimated from sonar range scans

Fig. 5. Sonar scans of the corridor of Fig. 4 and boundary of open space assumption

From sonar scan, depicted in Fig. 5 (a), actual RCDs were extracted, as shown in Fig. 6 (a). RCDs whose width is larger than 8° and difference in range data less than 2cm were collected. Simulated sonar readings and RCDs from them were obtained as shown in Fig. 6 (b). Total 6 of 8 actual RCDs appeared to be matching with simulated RCDs. Two target objects from two unmatched RCDs were registered in the line-corner map as target type unidentified objects. Line segments and corner points not observable by sonar were also registered in the map with mid-level belief. Their belief level can be updated with repeated observation in different position, which will be a further work of this study. Final belief reinforced line-corner map are shown in Fig. 8. Thicker lines distinguish line models that construct the matched wall or corner point. These lines and corner points would be helpful in selecting natural landmarks for future navigation problem.

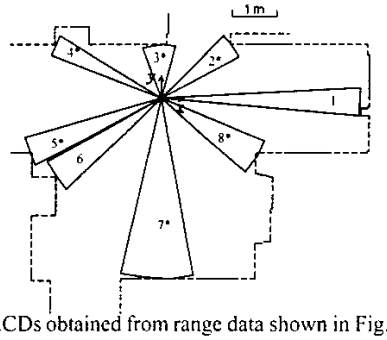

(a) RCDs obtained from range data shown in Fig. 5-(a)

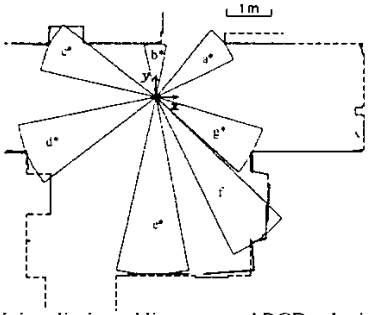

(b) Noise eliminated line map and RCDs obtained by simulated scan from the smoothed map

Fig. 6. RCDs obtained from actual sonar scan and RCDs predicted from smoothed line map generated by LSL Matching RCD pairs: (2, a), (3, b), (4, c), (5, d), (7, e), and (8, g)

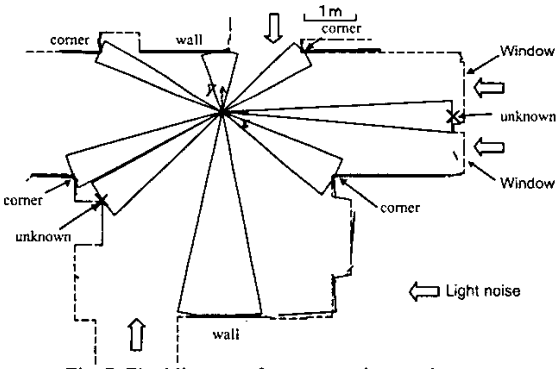

Fig. 7. Final line map from sensor integration: Belief reinforced objects are shown in thick lines.

V. CONCLUSION

An environment recognition method using sensor fusion of sonar sensor and laser structured light system is presented. LSL whose spatial resolution is much higher than sonar sensor plays a major role in achieving the line and corner model of the environment. However, fusing with sonar sensor could eliminate erroneous line models from light noise and restore missing object models, which cannot be achieved when only LSL is used. The effectiveness of the approach is demonstrated with experimental results.

References

[1] J. Leonard and H.F. Durrant-Whyte, "Directed sonar sensor for mobile robot navigation," Kluwer Academic Publishers, 1992.

[2] S. Yuta, S. Suzuki, Y. Saito and S. Iida, "Implementation of an active optical ranging sensor using laser slit for in-door intelligent mobile robot," Proc. IROS, pp. 415-420, 1991.

[3] I.S. Joung and H.S. Cho, "An active omni-directional range sensor for mobile robot navigation," IFAC J. of Control Engineering Practice, 1997.

[4] L. Matthies and A. Elfes, "Integration of sonar and stereo range data using a grid-based representation," Proc. IEEE Int. Conf. Rob. Auto., pp. 727-733, 1988.

[5] S.W. Bang, W. Yu and M.J. Chung, "Sensor-based local homing using omnidirectional range and intensity sensing system for indoor mobile robot navigation," Proc. IROS, pp. 542-548, 1995.

[6] Y. Goto and A. Stentz, "The CMU system for mobile robot navigation," Proc. IEEE Int. Conf. Rob. Auto., pp. 99-105, 1987.

[7] J. Vandorpe, H. Van Brussel and H. Xu, "LiAS: A reflexive navigation architecture for an intelligent robot system," IEEE Trans. Indust. Electron., vol. 43, no. 3, pp. 432-440, 1996.

[8] M. Kam, X. Zhu and P. Kalata, "Sensor fusion for mobile robot navigation," Proc. IEEE, vol. 85, no. 1, pp.108-119, 1997.

[9] P.L. Bogler, "Shafer-Dempster reasoning with applications to multisensor target identification systems," IEEE Trans. Sys. Man and Cyb., vol. SMC-17, no. 6, pp.968-977, 1987.

[10] A.P. Tirumalai, B.G. Schunck and R.C. Jain, "Evidential reasoning for building environment maps," IEEE Trans. Sys. Man and Cyb., vol. 25, no. 1, pp. 10-20, 1995.

[11] G. Dudek and P. Freedman, "Just-in-time sensing: efficiently combining sonar and laser range data for exploring unknown worlds," IEEE Int. Conf. Rob. Auto., pp. 667-671, 1996.

[12] A.M. Flynn, "Combining sonar and infrared sensors for mobile robot navigation," Int. J. Robot. Res., pp. 5-14, 1988.

[13] J. Gonzalez, A. Ollero and A. Reina, "Map building for a mobile robot equipped with a 2D laser rangefinder," Proc. IEEE ICRA, pp. 1904-1909, 1994.

[14] D.H. Ballard and C.M. Brown, *Computer Vision*, Prentice-Hall, Inc., 1982.

[15] G. Shafer, "A mathematical theory of evidence," Princeton University Press, 1976.

[16] R.C. Kuc and M.W. Siegel, "Physically based simulation model for acoustic sensor robot navigation," IEEE Trans. PAMI, vol. PAMI-9, no. 6, pp. 766-778, 1987.